CT machine geometry changes under thermal load

Benjamin A. Bircher[1], Felix Meli[1], Alain Küng[1], Rudolf Thalmann[1]

[1]Federal Institute of Metrology METAS, Laboratory for Length, Nano- and Microtechnology

Lindenweg 50, 3003 Bern-Wabern, Switzerland

e-mail: benjamin.bircher@metas.ch, felix.meli@metas.ch

Abstract

Computed tomography systems are increasingly used for dimensional metrology. Accurate CT machine geometry and temperatures close to 20 °C are crucial for dimensional measurements. Usually, considerable thermal loads are imposed onto CT systems by the X-ray source and the detector that dissipate heat in the order of 100 W. Because temperature variations and gradients induce deformations on the machine geometry, it is crucial to characterise and control such influences. Here, a home-built water cooling system for a flat-panel X-ray detector was characterised for heat dissipation into the CT system, positional and angular drift, and pixel grey value stability.

Keywords: CT machine geometry, thermal influences, geometry measurement system, metrology

1 Introduction

According to ISO 1 [1], the reference temperature for dimensional measurements is 20 °C. Since computed tomography (CT) systems are increasingly used for such measurements and contain major heat sources, especially in comparison to tactile coordinate measuring machines (CMMs), temperature control is highly relevant [2]. Key factors are a well-controlled absolute temperature of the object under investigation, as well as a stable CT system temperature, because temperature changes cause drift and thermal gradients that induce deformations. Such deformations deteriorate accurate reconstruction of the projection data that relies on a stable and well-known geometrical arrangement. Thermal studies were previously performed on X-ray tubes [3] and cabinet [4] temperatures. However, to our knowledge, no studies about the detector positon stability in relation to the temperature are available so far. The reason for this is probably the fact that the stability requirements on the detector are relatively low, since they correlate with the pixel size that is in the order of 0.1 mm. Here, we investigate the stability of a high-resolution flat-panel detector that imposes significant thermal load on the CT system, by monitoring temperature, position and pixel grey value stability.

2 X-ray flat-panel detector water cooling system

Figure 1, left shows the developed water-cooling system and shielding for the employed flat-panel detector (Perkin Elmer, XRD 1611 CP3, 4000 x 4000 pixels, nominal power dissipation 90 W). It consists of aluminium heat sinks in contact with a water-cooled copper tube. The water-conducting parts and detector electronics are lead-shielded to avoid scatter radiation and radiation damage. The detector assembly is mounted on an aluminium frame as shown in Figure 1, right. Calibrated NTC temperature sensors were distributed as follows: four in each corner of the detector aluminium heat sinks (detector housing, Figure 1, left), one on top and one in the base of the detector support structure (detector mount, Figure 1, right), one in the air above the rotary stage, and one at the air outlet of the radiation protection cabin. The water-cooling was adjusted to keep the heat flux into the CT system close to zero. That is, the air outlet temperature baseline was measured with the detector being switched off. Subsequently, the detector was switched on and the water temperature tuned until the cabin outlet air temperature reached baseline again. This resulted in a standard thermostat setpoint temperature of 16 °C and an average detector temperature of (19.0 ± 0.6) °C.

3 Temperature, position and image stability analysis

3.1 Temperatures and thermal time constants

First, the temperatures and thermal time constants for air- and water-cooling of the detector were evaluated. Figure 2 shows time series of the temperature of the detector housing, the detector mounting structure, and the air. The temperatures in equilibrium are provided in Table 1. At standard thermostat setpoint (T_{set} = 16 °C), no temperature gradient was observed across the detector mounting structure, indicating no heat flux into it. The temperature gradient across the detector housing (1.1 °C) is mainly caused by the spatial distribution of the electronics. As soon as the thermostat setpoint is increased, heat starts to flow into the detector mount resulting in a temperature gradient across it. After the water-cooling is entirely switched off, the detector is only air-cooled and reaches an average temperature of 28.9 °C with a gradient of 2.2 °C. The air temperature above the rotary stage, i.e. sample position, only increases by 0.4 °C, indicating a sufficiently high air velocity to dissipate the generated heat at sample position.
The thermal time constants were determined by fitting exponential curves to the temperature series. The time constant of the detector housing (time to reach 63.2 % of the equilibrium temperature) was about 59 min for air-cooling and 9 min for water-

cooling. In contrast to the detector housing, the thermal time constants of the detector mount were significantly longer: about 94 min and 53 min for air- and water-cooling, respectively. This corroborates the strategy to avoid heat flux into the detector mount, to avoid long warm-up periods.

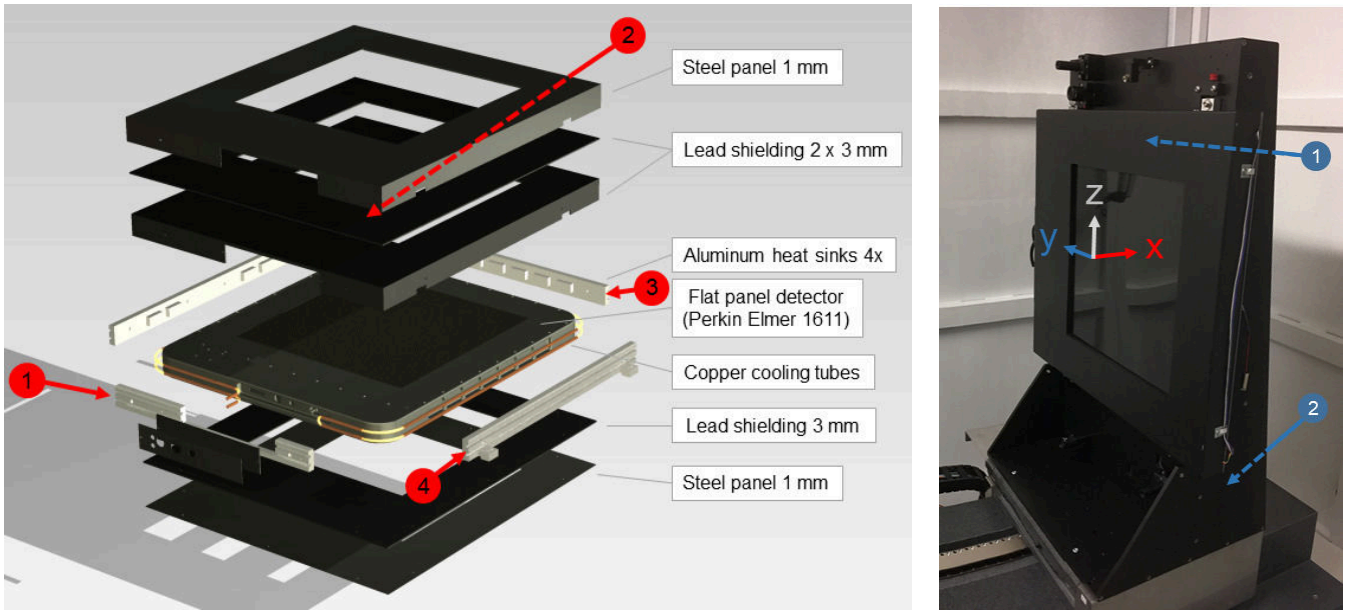

Figure 1: Left: CAD of the flat-panel detector cooling and shielding system in exploded view. The numbers indicate the positions of four detector housing temperature sensors. Right: Photo of the shielded and water-cooled flat-panel detector mounted on an aluminium supporting frame. The numbers indicate the positions of two detector mount temperature sensors.

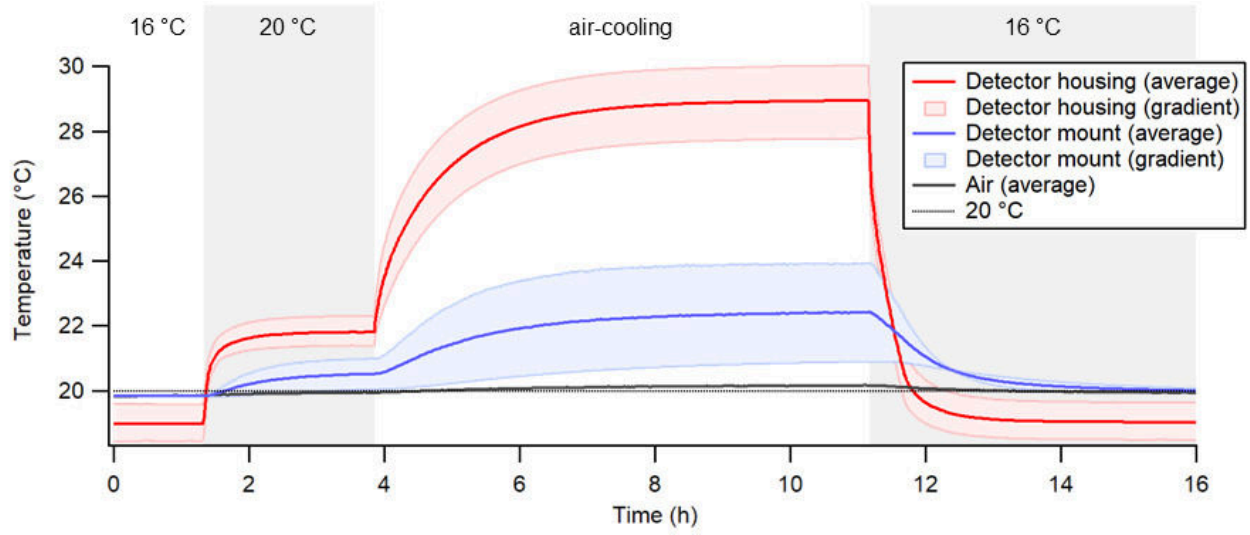

Figure 2: Detector housing (red) and mounting structure (blue) temperatures and air temperature (black) under different cooling strategies: Water-cooling 16 °C (no heat transfer into the CT system) and 20 °C, and air-cooling. Temperature sensor positions are indicated in Figure 1.

Table 1 : Equilibrium temperatures for different cooling strategies. A thermostat setpoint of T_{set} = 16 °C, results in zero heat transfer into the CT system (baseline).

Cooling strategy	Air temperature (°C)	Temperature detector housing		Temperature detector mount	
		Average (°C)	Gradient (°C)	Average (°C)	Gradient (°C)
Water-cooling (T_{set} = 16 °C)	19.8	19.0	1.1	19.8	0.0
Water-cooling (T_{set} = 20 °C)	19.9	21.8	0.9	20.5	0.9
Passive air-cooling	20.2	28.9	2.2	22.4	3.0

3.2 Position variations

Detector positional drift results in blurred CT data [5] and deteriorates its geometrical integrity. A stability of 1/10 of a pixel is an appropriate target, because below the uncertainties of other effects become dominant (e.g. edge detection). Since temperature variations and gradients cause instrument geometry deformations, the 6 degrees of freedom (3 translations, 3 rotation angles) of the flat-panel detector were measured relative to the detector centre during temperature cycles. To this end, the previously developed geometry measurement system, which consists of interferometers and straightness sensors, installed on METAS-CT, was employed [6].

Figure 3 shows the temperature curves and the corresponding detector movements in absolute units and relative to the pixel size of 0.1 mm. The translational and angular movements correlate with the detector housing and mount temperatures. The largest displacement was observed in vertical (z) direction and is accounted to the thermal expansion of the aluminium detector mount. Horizontal displacements (x and y) are mainly attributed to the angular deviations, with the centre of rotation being at the base of the detector mount. The observed angular deviations remained very small, i.e. less than 1/10 of a pixel across the detector width. Their cause is asymmetrical mounting of the detector and gradients in the mounting structure. The consequence of shifting temperature gradients is deformation of the detector mount, resulting in a bend in the detector pitch curve, observed after every setpoint adjustment.

In summary, the detector movements under water-cooling remain below 1/10 of a pixel. Therefore, no warm-up period is required to remain within the positional stability tolerance.

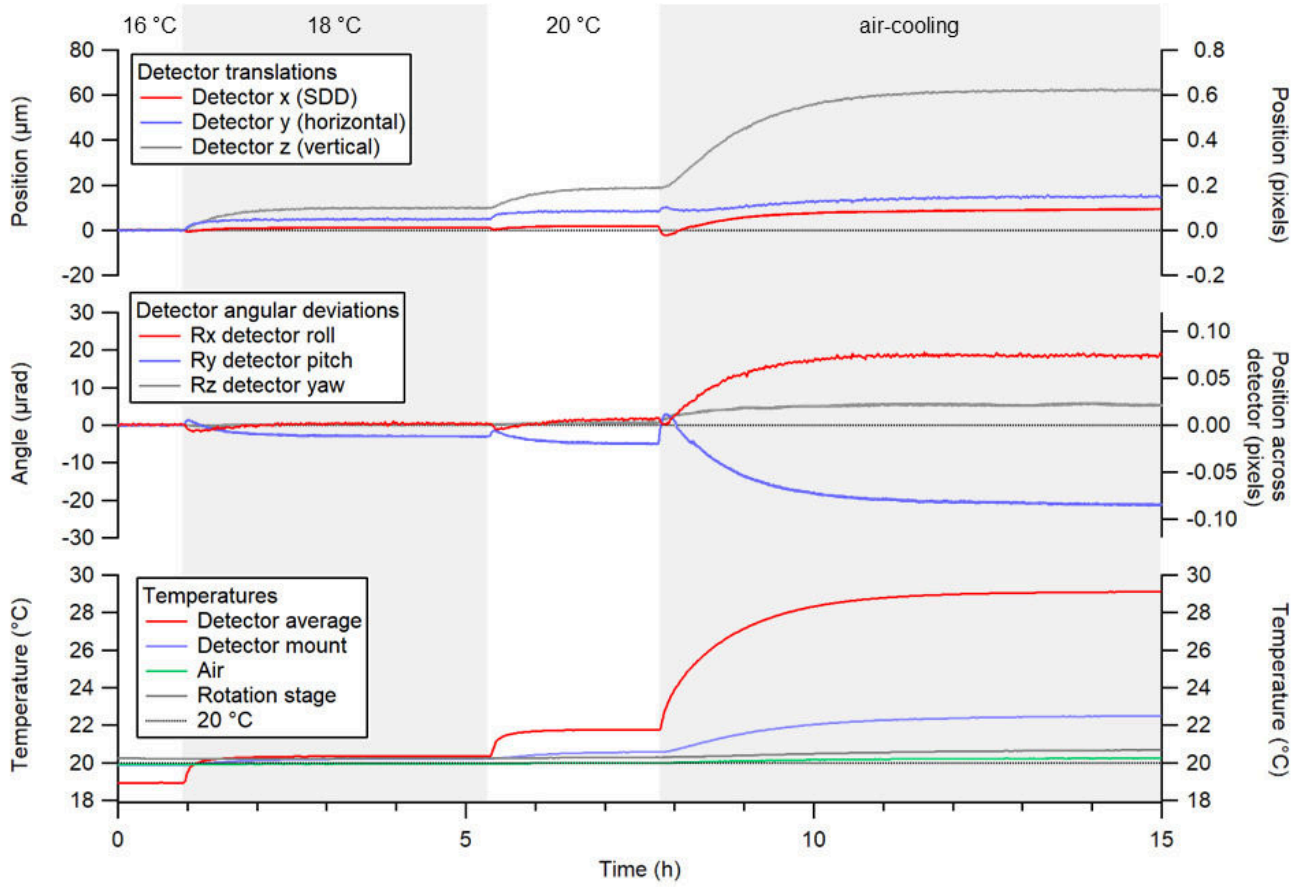

Figure 3: Detector position (top), angular deviations (middle), and CT system temperatures (bottom) under different cooling settings (thermostat setpoints: water-cooling 16 °C (baseline; no heat transfer into the CT system), 18 °C, 20 °C and air-cooling); see Figure 1, right for coordinate system.

3.3 Pixel grey value

Flat-panel detectors respond to temperature changes with changes in pixel offsets (dark currents) and sensitivities (gains) [7]. Since changes in these parameters introduce ring artefacts [5] and, thus, deteriorate image quality, it is essential to stabilise them. To investigate this effect, water-cooling setpoints were cycled from 16 °C to 20 °C in 1 °C steps and finally the water-cooling was switched off. An offset image, without X-ray exposure, was recorded every minute during temperature cycling. A baseline image, calculated from 100 images at 16 °C water-cooling, was subtracted from all images before analysis. Subsequently, average (offset) and standard deviation (spread) of the pixel grey values across the detector (4000 x 4000 pixels, 16-bit converter with 65536 gray values) of 50 projections were averaged for each cooling setting.

The results are shown in Figure 4. In the observed range, the detector offset expresses a quadratic behaviour to the average detector temperature. It increases by about 800 grey values (GV) when warming up under air-cooling. This is about 10 % of the grey value in highly absorbing regions and could introduce considerable density variations in the projection images. The grey value standard deviation seems to originate mainly from the temperature gradient across the detector. It rises from 19 GV (0.03 % of the dynamic range) under 16 °C water-cooling to 131 GV (0.2 %) under air-cooling. Furthermore, the grey value distribution becomes skewed due to the variance in pixel sensitivities, at higher temperatures. Such variations in pixel sensitivity introduce ring artefacts in the data, especially when working with highly absorbing samples.

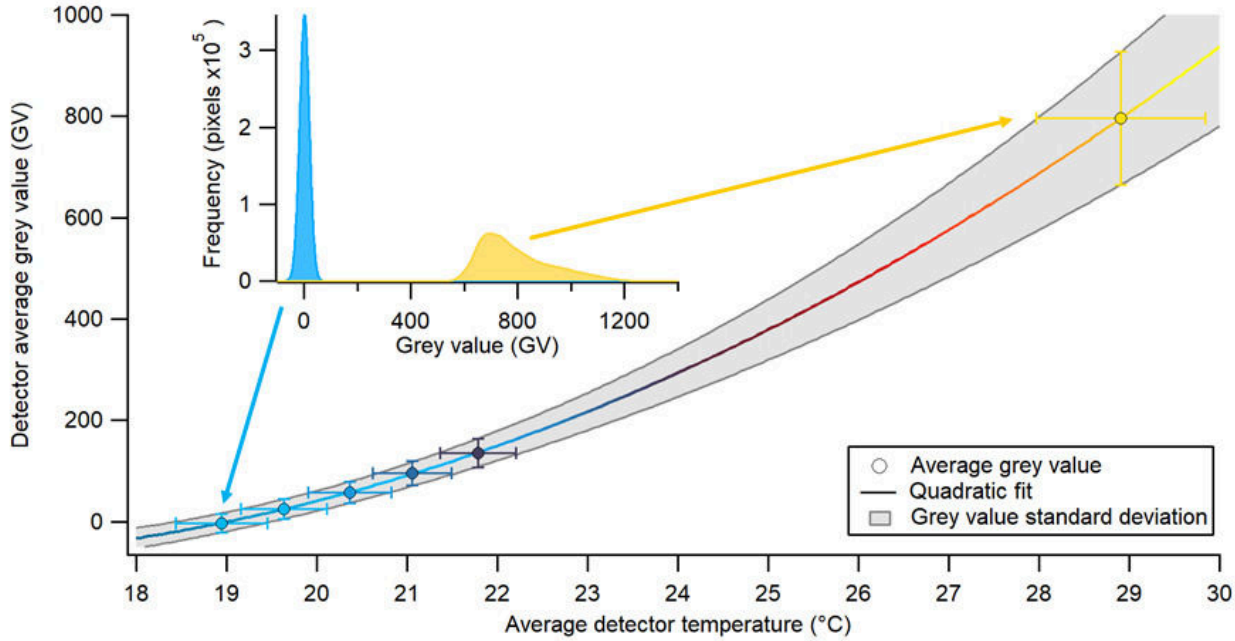

Figure 4: Average dark grey value across all detector pixels relative to the detector average temperature; error bars indicate grey value (vertical) and temperature (horizontal) standard deviations across the detector. The following cooling settings were used: Water-cooling setpoints 16 °C to 20 °C in 1 °C steps, and air-cooling. The inset shows the grey value histogram for water-cooling at 16 °C (blue) and air-cooling (yellow).

4 Conclusions

We analysed the consequences of heat dissipation into a CT system, originating from a flat-panel detector, by monitoring temperatures, position and pixel grey values. It is emphasised that results were obtained on the custom-built METAS-CT [6] and depend on the specific CT system design. However, they can be generalised in a qualitative manner.

We developed an efficient, shielded detector water-cooling system that keeps the detector average temperature at 19 °C, whereas temperature rises to 29 °C without active water-cooling. The cooling power was adjusted to minimise the net heat transfer into the CT system. We observed no temperature gradient across the detector mount, confirming negligible heat flux into it. This is advantageous since any heat flux reaching the granite base of our machine, which has very large thermal inertia, would result in uncontrolled long-term drifts. Next, thermal time constants were compared for water- and air-cooling. To reach 95 % of the equilibrium temperature, a warm-up period of three time constants is required. Thus, the time to reach operational readiness after system start-up was six-fold reduced employing water-cooling (from 3 h to 0.5 h). Furthermore, under water-cooling positional drifts remained below 0.1 pixels in all directions from the beginning, rendering a warm-up period redundant.

The main advantage of an optimised detector water-cooling system is not only minimal heat flow into the system and stable thermal and geometrical conditions, but also strongly reduced start-up times and stable detector dark currents and pixel gains. Furthermore, water-cooling is much less susceptible to changes in thermal load compared to air-cooling. After warm-up, i.e. in thermal equilibrium, the detector position stability (below 0.1 pixel) and the pixel gray value stability (SD << 0.1 %) is sufficient for high-resolution CT scans.

In a future study, the thermal loads of the X-ray tube will be investigated. Since the X-ray tube position stability should be on the order of 1/10 of a voxel, i.e. 0.1 µm for high-resolution CT scans, the requirements are more stringent than for the detector. Furthermore, the versatile operation modes of the X-ray tube pose high variations in thermal load and, thus, high demands on the cooling system.

Acknowledgements
This work is part of the European Metrology Programme for Innovation and Research (EMPIR) project 17IND08 AdvanCT. The EMPIR initiative is co-funded by the European Union's Horizon 2020 research and innovation programme and the EMPIR participating states.

References

[1] ISO/TC 213, "ISO 1:2016 Geometrical product specifications (GPS) -- Standard reference temperature for the specification of geometrical and dimensional properties," 2016.
[2] J. P. Kruth, M. Bartscher, S. Carmignato, R. Schmitt, L. De Chiffre, and A. Weckenmann, "Computed tomography for dimensional metrology," *CIRP Ann. - Manuf. Technol.*, vol. 60, no. 2, pp. 821–842, 2011.
[3] N. Flay, W. Sun, S. Brown, R. Leach, and T. Blumensath, "Investigation of the Focal Spot Drift in Industrial Cone-beam X-ray Computed Tomography," *Digit. Ind. Radiol. Comput. Tomogr.*, no. June, pp. 22–25, 2015.
[4] J. Hiller, M. Maisl, and L. M. Reindl, "Physical characterization and performance evaluation of an x-ray micro-computed tomography system for dimensional metrology applications," *Meas. Sci. Technol.*, vol. 23, no. 8, p. 085404, 2012.
[5] G. R. Davis and J. C. Elliott, "Artefacts in X-ray microtomography of materials," *Mater. Sci. Technol.*, vol. 22, no. 9, pp. 1011–1018, 2006.
[6] B. A. Bircher, F. Meli, A. Küng, and R. Thalmann, "A geometry measurement system for a dimensional cone-beam CT," in *8th Conference on Industrial Computed Tomography, Wels, Austria (iCT 2018)*, 2018.
[7] J. H. Siewerdsen and D. A. Jaffray, "A ghost story: Spatio-temporal response characteristics of an indirect- detection flat-panel imager," *Med. Phys.*, vol. 26, no. 8, pp. 1624–1641, 1999.